MEDWIN PUBLISHERS
Committed to Create Value for Researchers

International Journal of Zoology and Animal Biology
ISSN: 2639-216X

Towards a Testable Cybernetic Model of Hydrodynamic Signal Filtering in the Teleost Lateral Line

Boblique J*

Independent Researcher, Founder of Science 4.0, France

***Corresponding author:** Julien Boblique, Independent Researcher, Founder of Science 4.0, France

Short Communication

Volume 9 Issue 6

Received Date: October 26, 2026

Published Date: November 05, 2026

DOI: 10.23880/izab-16000705

Abstract

The mechanosensory lateral line enables fishes to detect hydrodynamic signals arising from external sources and self-generated locomotor movements. Although the mechanical properties of neuromasts and the inhibitory effects of cholinergic efferent regulation have been investigated experimentally, the relationship between correlated hydrodynamic noise, sensory gain modulation, and metabolic expenditure remains an important modeling problem.

Within the Science 4.0 framework, this theoretical perspective proposes a falsifiable cybernetic model integrating superficial and canal neuromast transfer functions, spatial noise correlations, efferent attenuation, and simplified synaptic resource dynamics.

The framework distinguishes established biological evidence [D], theoretical assumptions [H], analytical consequences [C], and experimental validation requirements [E].

We derive conditional predictions concerning the limitations imposed by correlated hydrodynamic noise, the effects of efferent suppression on instantaneous signal-to-noise ratio (SNR), and potential trade-offs between post-locomotor sensory recovery and metabolic expenditure.

The proposed relationships are not presented as experimentally validated mechanisms. They provide a quantitative starting point for testing the interaction between hydrodynamic sensing, neural feedback, and energetic constraints in fish lateral-line systems.

Keywords: Teleost Lateral Line; Mechanotransduction; Neuromasts; Hydrodynamic Filtering; Correlated Noise; Cholinergic Efferent Control; Bioenergetics; Science 4.0

Introduction and Epistemological Scope

The lateral-line system allows aquatic vertebrates to detect water movements generated by prey, predators, obstacles, environmental currents, and their own locomotion [1].

Its sensory function involves mechanical filtering, cellular transduction, neural encoding, and central modulation.

These mechanisms constitute a useful biological context for examining interactions between fluid dynamics, information processing, and non-equilibrium energy expenditure.

Within the Science 4.0 framework, we propose that the lateral line can be investigated as a distributed sensory system whose performance depends on both peripheral mechanics and activity-dependent neural regulation.

However, established biological phenomena must be distinguished from new mathematical hypotheses.

Accordingly, this study adopts four epistemological categories:

[D] Established data: Experimental observations reported in the scientific literature.

[H] Model hypotheses: Simplifying assumptions and proposed mathematical relationships requiring justification.

[C] Calculated consequences: Analytical predictions derived from explicitly stated assumptions.

[E] Experimental validation: Measurements or interventions required to assess the proposed predictions.

The objective is not to claim a newly discovered physiological mechanism, but to formulate a quantitative model that can be challenged by experimental evidence.

Dual-Modality Hydrodynamic Transfer Functions

Established Biological Foundations [D]

Teleost lateral-line systems include superficial neuromasts (SNs), exposed to external water movement, and canal neuromasts (CNs), located within fluid-filled canals connected to the external environment through pores.

Superficial neuromasts respond to local fluid motion through fluid–structure interactions involving the cupula and sensory hair bundles.

Canal neuromasts respond to pressure differences driving fluid movement within the canals. Their responses depend on canal geometry, fluid inertia, viscous resistance, and stimulus frequency [1,2].

The two receptor classes therefore exhibit different hydrodynamic filtering properties.

Proposed Transfer-Function Model [H]

For a linearized small-amplitude regime, let:

- $U_\infty(\omega)$ denote the Fourier amplitude of an externally defined fluid-velocity stimulus, in m/s.
- $X_k(\omega)$ denote the corresponding cupular displacement, in metres.
- $H_k(\omega) = X_k(\omega)/U_\infty(\omega)$ denote the transfer function, with units of seconds.
- $k \in \{SN, CN\}$ identify the receptor class.

We introduce the following phenomenological transfer functions:

Superficial neuromasts

$$H_{SN}(\omega) = \frac{K_{SN} B_{bl}(\omega)}{D_{SN}(\omega)}$$

Canal neuromasts

$$H_{CN}(\omega) = \frac{K_{CN}(i\omega\tau_c)}{D_{CN}(\omega)}$$

where:

$$D_k(\omega) = \left(1 - \frac{\omega}{\omega_k}\right)^2 + 2i\zeta_k\left(\frac{\omega}{\omega_k}\right)$$

Here:
K_{SN} and K_{CN} are dimensional transfer coefficients, in seconds.
$B_{bl}(\omega)$ is a dimensionless boundary-layer transfer factor.
τ_c is a characteristic canal response time, in seconds.
ω_k represents a characteristic angular frequency, in rad/s.
ζ_k is a dimensionless effective damping ratio.

This formulation is dimensionally consistent because both transfer coefficients H_k have units of seconds.

For an oscillatory viscous boundary layer, a characteristic thickness is:

$$\delta\nu(\omega) = \sqrt{(2\nu/\omega)},$$

where ν is the fluid kinematic viscosity. The detailed dependence of B_bl on geometry and frequency must be determined from an appropriate fluid–structure model or measured experimentally.

The $i\omega\tau_c$ term provides an idealized low-frequency attenuation mechanism for the canal pathway. It does not imply that canal-neuromast behavior is universally described by a pure acceleration detector.

These equations are reduced-order hypotheses rather than constitutive laws already validated for every teleost species.

Proposed test [E]: Estimate the transfer parameters by comparing controlled water-velocity stimuli with cupular displacement measurements across frequency.

Copyright© Boblique J.

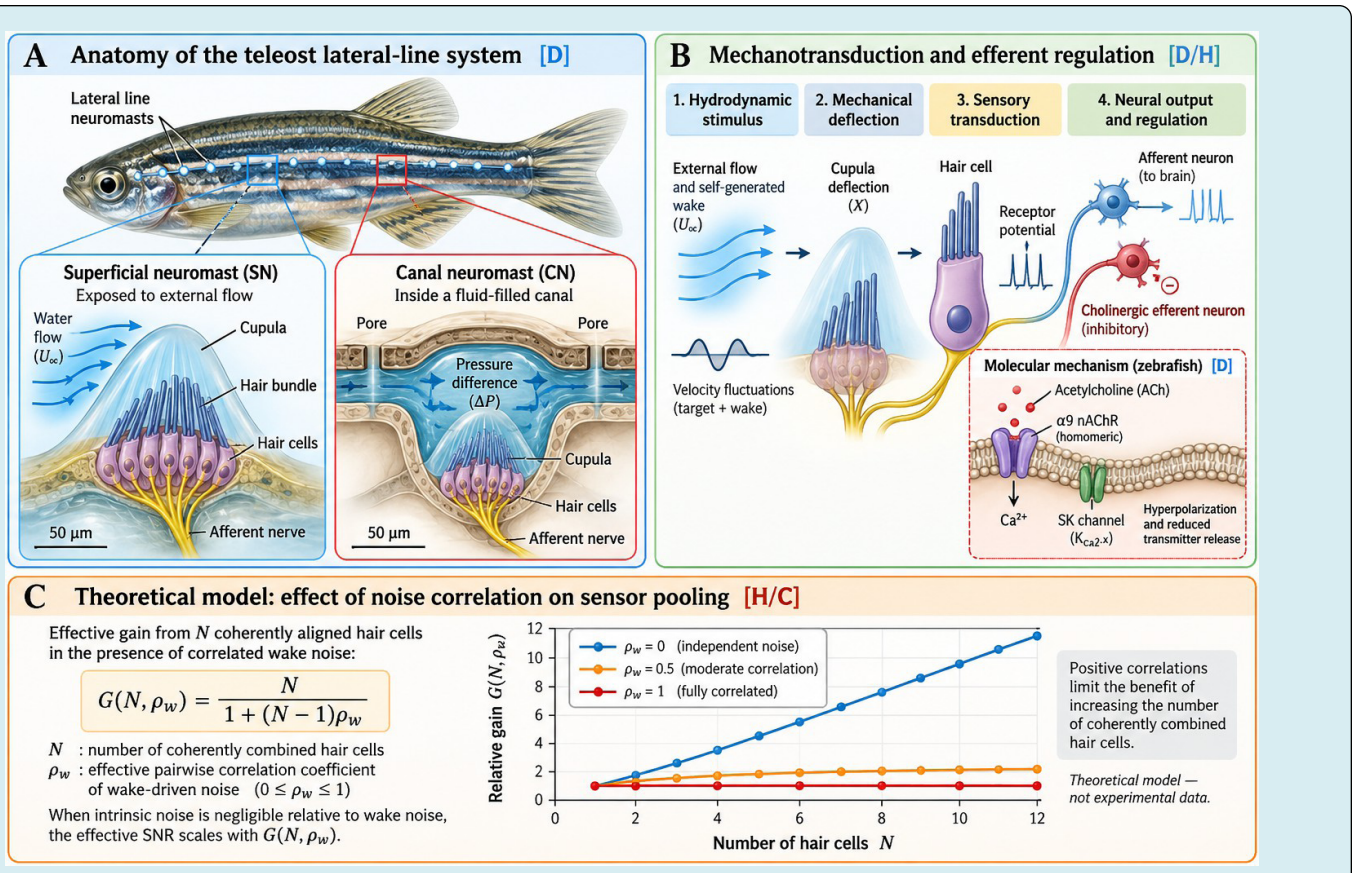


Figure 1: Anatomical organization, mechanotransduction, and theoretical noise-correlation model of the teleost lateral-line system.

Anatomical organization [D]: Schematic representation of the teleost lateral-line system, illustrating superficial neuromasts (SNs), exposed to external water flow, and canal neuromasts (CNs), responding to pressure differences within fluid-filled canals.

Mechanotransduction and efferent regulation [D/H]: Simplified representation of hydrodynamic stimulation, cupular deflection, hair-cell sensory transduction, afferent signaling, and inhibitory cholinergic efferent modulation. The molecular inset illustrates α9-containing nicotinic acetylcholine receptor signaling coupled to SK potassium channels, as investigated in zebrafish.

Theoretical prediction [H/C]: Effective sensor-pooling gain, G(N, ρw) = N/[1 + (N − 1)ρw], as a function of the number of coherently combined hair cells (N), for three assumed wake-noise correlation coefficients (ρw = 0, 0.5, and 1). The model predicts that positive noise correlations limit the benefit of increasing sensor number when intrinsic noise is negligible.

Scientific status: Panels A and B are conceptual schematic representations, not to scale. Panel C presents analytical model predictions, not experimental measurements.

Correlated Hydrodynamic Noise and Efferent Regulation

Biological Basis [D]

Hair cells convert mechanical deflection into electrical and synaptic signals. Measurements in zebrafish demonstrate heterogeneous mechanical sensitivities and response dynamics across hair cells within a neuromast [3].

Cholinergic efferent pathways modulate lateral-line sensitivity during locomotion.

In zebrafish, experiments support an inhibitory mechanism involving α9-containing nicotinic acetylcholine receptors and small-conductance calcium-activated potassium channels [4].

The available evidence supports functional homomeric α9 receptors in the investigated zebrafish system. This mechanism should not automatically be generalized to every species or developmental stage.

Copyright© Boblique J.

Experiments also show that efferent inhibition can be selective for particular hair-cell orientations rather than uniformly suppressing all sensory responses [5].

These findings motivate the introduction of an activity-dependent gain-control variable.

Model of Correlated Sensory Noise [H]

Consider an effectively aligned population of N sensory hair cells contributing coherently to detection of a selected hydrodynamic stimulus.

Let:

- $S_{ext}(\omega)$ represent the external target-velocity power spectral density.
- $S_{wake}(\omega)$ represent the self-generated wake-velocity power spectral density.
- $S_{int}(\omega)$ represent the intrinsic, uncorrelated output-equivalent noise spectrum.
- $\rho_w(\omega)$ represent an effective pairwise wake-noise correlation coefficient.
- $\gamma(t) \in (0,1]$ represent efferent gain attenuation.
- $r(t) \in [0,1]$ represent the fraction of available synaptic transmission resources.

For a simplified population with equal weighting, coherent target responses, and equal positive pairwise wake-noise correlations, we propose:

$$SNR_{eff}^{(k)}(\omega,t) = \frac{N^2(\gamma r)^2 |H_k(\omega)|^2 S_{ext}(\omega)}{N S_{int}(\omega) + N\left[1+(N-1)\rho_w(\omega)\right](\gamma r)^2 |H_k(\omega)|^2 S_{wake}(\omega)}$$

The hydrodynamic signal and wake spectra are expressed in compatible velocity-squared spectral units. Multiplication by $|H_k(\omega)|^2$ converts them to output-equivalent displacement spectra.

This approximation assumes that intrinsic noise is independent between the selected cells and is not attenuated by the same gain factor.

The range $0 \le \rho_w \le 1$ is adopted for the positive-correlation case. More general sensory populations require a full covariance matrix and cell-specific weighting.

These assumptions must be tested rather than inferred solely from neuromast anatomy.

Analytical Consequence: Correlated-Noise Limitation [C1]

When intrinsic noise is negligible relative to hydrodynamic wake noise, the proposed SNR tends toward:

$$SNR_{eff} = \left[\frac{N}{1+(N-1)\rho_w}\right]\left[\frac{S_{ext}}{S_{wake}}\right].$$

For illustration, if N = 10 and $\rho_w = 0.5$:

$$\frac{N}{1+9\times 0.5} \approx 1.82$$

In contrast, an idealized uncorrelated population with $\rho_w = 0$ would yield a factor of 10.

Thus, within this model, positively correlated wake interference limits the improvement obtained by increasing the number of coherently combined cells.

This result is an analytical consequence of the assumed covariance structure, not a measured gain in living fish.

Efferent Attenuation and Instantaneous SNR [C2]

The proposed expression also shows that reducing γ does not necessarily improve instantaneous SNR. If the same gain factor attenuates both external signals and wake-related responses while intrinsic noise remains unchanged, decreasing γ lowers instantaneous SNR whenever intrinsic noise is nonzero.

Consequently, the potential biological benefit of efferent inhibition may lie in preserving dynamic range, limiting excessive synaptic activity, restructuring direction-selective information, or improving later sensory availability.

These possibilities are not mathematically equivalent and require separate tests.

Synaptic Resource Dynamics and Metabolic Constraints

Proposed Recovery Model [H]

To represent activity-dependent resource depletion, let r(t) denote a normalized available synaptic resource fraction. We introduce:

$$\frac{dr}{dt} = \frac{1-r}{\tau_{rec}} - \left[\frac{\gamma(t)R_0(W)}{V_{pool}}\right]r$$

where:

τ_{rec} is an effective resource-recovery time, in seconds.

$R_0(W)$ is a hypothetical unsuppressed vesicular demand rate, in vesicles/s per cell.

V_{pool} is an effective resource capacity, in vesicles.

Copyright© Boblique J.

W denotes locomotion-related sensory drive.

The model assumes that stronger efferent attenuation can reduce resource consumption during a locomotor burst.

This interpretation is a hypothesis and does not establish that depletion prevention is the actual biological function of cholinergic inhibition.
For constant γ and W, the model has the solution:

$$r(t) = r_{ss} + [r(0) - r_{ss}] \exp\left[-\left(\frac{1}{\tau_{rec}} + \frac{\gamma R_0}{V_{pool}} \right) t \right], \text{ with: } r_{ss} = \frac{1}{1 + \frac{\gamma \tau_{rec} R_0}{V_{pool}}}.$$

For otherwise identical conditions, lowering γ reduces the model's resource-depletion term. A subsequent improvement in sensory recovery would depend on how resource availability affects neural response amplitude and noise. No universal post-burst recovery time is assumed.

Bioenergetic Cost Function [H]

We propose the following simplified power balance:

$$P_{met}(t) = N\left[P_{basal} + \varepsilon_v \gamma(t) r(t) R_0(W) + c_{eff}\left(1 - \gamma(t)\right) \right],$$

where:
P_{basal} is basal metabolic power per cell, in watts.
ε_v is the effective energy expenditure per vesicle processed, in joules/vesicle.
$\gamma r R_0$ is the effective modeled vesicular processing rate, in vesicles/s.
c_{eff} is a phenomenological maximum efferent-control power cost per cell, in watts.

The expression includes basal expenditure, activity-dependent synaptic expenditure, and a simplified cost associated with inhibitory control. It does not claim to constitute a complete biochemical ATP budget. Ionic pumping, calcium handling, neurotransmitter recycling, and other processes would require additional mechanistic characterization.

Conditional Energetic Threshold [C3]

Comparing inhibited and uninhibited states at the same resource fraction r and sensory drive W gives:

$$\Delta P_{met} = N(1-\gamma)\left[c_{eff} - \varepsilon_v r R_0(W) \right].$$

Accordingly, within these assumptions, reducing gain decreases the modeled instantaneous metabolic power when:

$$\varepsilon_v r R_0(W) > c_{eff}$$

This condition is not an experimentally established threshold of wake intensity. A corresponding wake-intensity threshold can be inferred only after establishing an appropriate relationship between sensory drive W and the vesicular demand function $R_0(W)$. Moreover, allowing r to evolve differently between inhibited and uninhibited states requires a time-dependent energy comparison rather than the instantaneous expression alone. The distinction is important because energy savings, information preservation, and recovery speed are separate quantities.

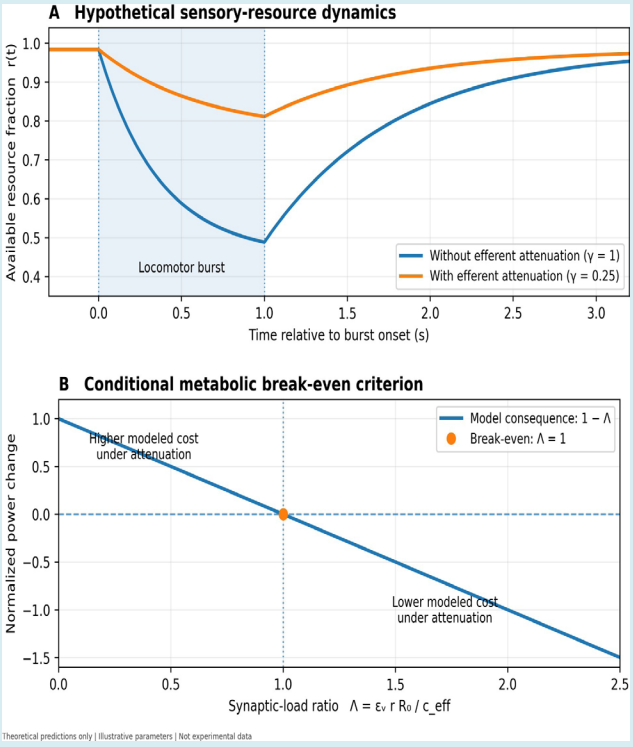


Figure 2: Theoretical sensory-resource dynamics and conditional bioenergetic trade-offs during efferent regulation.

Synaptic resource dynamics [H/C]. Simulated evolution of normalized available sensory resources, r(t), during a one-second locomotor burst and subsequent recovery. Two hypothetical conditions are compared: absence of efferent attenuation (γ = 1) and efferent attenuation during locomotion (γ = 0.25). Illustrative parameters are τ_{rec} = 0.8 s, V_{pool} = 100 vesicles, resting demand R_0 = 2 vesicles/s, and locomotor demand R_0 = 150 vesicles/s. Both conditions return to γ = 1 after the burst.
Conditional metabolic break-even [H/C]. Normalized instantaneous metabolic-power difference between attenuated and unattenuated conditions, evaluated at fixed

Copyright© Boblique J.

sensory resource availability and sensory drive. Defining $\Lambda = \frac{\varepsilon_v r R_0}{c_{\text{eff}}} \Rightarrow \frac{\Delta P_{\text{met}}}{N(1-\gamma)c_{\text{eff}}} = 1 - \Lambda$. The modeled break-even condition occurs at $\Lambda = 1$. Values above this threshold indicate lower modeled metabolic power under attenuation, conditional on the stated assumptions.

Scientific status: Both panels represent analytical calculations from a hypothetical reduced-order model. Parameter values are illustrative and have not been experimentally identified. The figures do not establish biological recovery times or measured ATP savings.

Falsifiable Predictions and Experimental Strategy

The proposed framework yields three principal questions suitable for experimental confrontation.

Prediction P1-Correlated-Noise Limitation [C/E]

For matched stimulus statistics and neural recording conditions, stronger positive cross-correlations between wake-driven sensory outputs should reduce the effective benefit of pooling additional similarly oriented hair cells.

This prediction can be tested by estimating sensory response covariance matrices under controlled flow stimulation.

Prediction P2-Gain Modulation and Recovery [C/E]

Under comparable locomotor stimulation, efferent inhibition may reduce peak synaptic demand and modify post-burst response recovery. A measurable prediction requires independent estimates of gain suppression γ, response availability r, and recovery dynamics. The hypothesis would be challenged if efferent manipulation produces no reproducible relationship between modeled resource availability and subsequent sensory responses. No recovery time below 20 ms is asserted.

Prediction P3-Energetic Trade-off [C/E]

An energetic benefit from efferent attenuation should occur only in regimes where the reduction in activity-dependent expenditure exceeds the additional cost of control. This prediction requires measurements or defensible estimates of synaptic activity, ion-transport expenditure, and cellular energetic state.

Proposed Experimental Approach

A first experimental program could use zebrafish lateral-line preparations to combine controlled hydrodynamic stimulation, cupular deflection measurements, afferent activity, calcium imaging, and indicators of synaptic glutamate release. Comparisons between spontaneous or induced locomotor activity and controlled efferent perturbations could help distinguish externally generated signals from motor-related sensory feedback. Where technically feasible, metabolic indicators could be investigated alongside electrophysiological recordings.

Control conditions should include changes in stimulus amplitude, frequency, hair-cell orientation, and efferent activity.

Because superficial and canal neuromasts differ in morphology and developmental availability, their transfer functions should be validated in appropriate preparations rather than assuming that both can be characterized identically in very young zebrafish larvae.

Parameter fitting should include uncertainty intervals, assessment of parameter correlations, and comparison with simpler competing models. This is essential to distinguish an identifiable physiological mechanism from a mathematically flexible description [6,7].

Conclusion

The teleost lateral-line system offers a biological example of interacting hydrodynamic, mechanical, neural, and energetic processes. The present theoretical perspective proposes a reduced-order cybernetic framework linking neuromast transfer functions, correlated sensory noise, efferent gain regulation, synaptic resource dynamics, and metabolic expenditure. Three analytical consequences emerge under explicit assumptions: correlated interference can limit the benefits of sensor pooling; efferent suppression does not automatically improve instantaneous SNR; and metabolic savings depend on the balance between activity-dependent expenditure and regulatory cost. These results are conditional properties of a proposed mathematical model, not experimental demonstrations of physiological optimization. The principal contribution is therefore a set of measurable quantities and falsifiable relationships that can guide subsequent investigation.

Within Science 4.0, this approach illustrates a general methodological principle: biological resilience should be investigated through explicit physical definitions, measurable mechanisms, uncertainty analysis, and experimentally

Copyright© Boblique J.

testable predictions rather than inferred from qualitative analogies alone.

Declaration of Study Status

This manuscript presents a theoretical framework and analytical predictions. No new biological experiments or experimental validation of the proposed model are reported. Numerical parameters introduced in future implementations must be independently justified or explicitly identified as illustrative assumptions.

References

1. Mogdans J (2019) Sensory ecology of the fish lateral-line system: Morphological and physiological adaptations for the perception of hydrodynamic stimuli. Journal of Fish Biology 95(1): 53-72.

2. McHenry MJ, Strother JA, van Netten SM (2008) Mechanical filtering by the boundary layer and fluid–structure interaction in the superficial neuromast of the fish lateral line system. Journal of Comparative Physiology A 194(9): 795-810.

3. Pichler P, Lagnado L (2019) The transfer characteristics of hair cells encoding mechanical stimuli in the lateral line of zebrafish. The Journal of Neuroscience 39(1): 112-124.

4. Carpaneto Freixas AE, Moglie MJ, Castagnola T (2021) Unraveling the molecular players at the cholinergic efferent synapse of the zebrafish lateral line. The Journal of Neuroscience 41(1): 47-60.

5. Pichler P, Lagnado L (2020) Motor behavior selectively inhibits hair cells activated by forward motion in the lateral line of zebrafish. Current Biology 30(1): 150-157.

6. Lunsford ET, Skandalis DA, Liao JC (2019) Efferent modulation of spontaneous lateral line activity during and after zebrafish motor commands. Journal of Neurophysiology 122(6).

7. Boblique J (2026) Science 4.0: Integrating biophysical signal optimization, non-equilibrium thermodynamics, and hydrodynamic boundary constraints in living systems architecture. Biomedical Journal of Scientific & Technical Research 66(4): 58936-58940.

Copyright© Boblique J.

YOUR RESEARCH DESERVES GLOBAL VISIBILITY

• Publish • Discover • Share • Connect

MEDICAL	CLINICAL	LIFESCIENCES	PHARMA
90+ OPEN ACCESS JOURNALS		400+ RESEARCH TOPICS	

SUBMIT YOUR RESEARCH
Submit your manuscript through our online submission system.

REPRINTS
If you require a reprint of any article, please contact us.
info@medwinpublishers.com

BECOME A REVIEWER
Share your expertise and contribute to scholarly publishing.

SCAN TO EXPLORE MEDWIN JOURNALS

• Journals • Submit Manuscript • Reviewer Program • Article Tracking

Our Journals indexed in

Embase® ELSEVIER | PubMed National Library of Medicine NLM | Crossref | Google Scholar | INDEX COPERNICUS INTERNATIONAL | ISSN INTERNATIONAL STANDARD SERIAL NUMBER INTERNATIONAL CENTRE | ROAD DIRECTORY OF OPEN ACCESS SCHOLARLY RESOURCES

EuroPub | Scilit | WorldCat® | Academic Resource Index ResearchBib | ADVANCED SCIENCE INDEX | INTERNATIONAL Scientific Indexing | ICMJE INTERNATIONAL COMMITTEE of MEDICAL JOURNAL EDITORS

This article published by **Medwin Publishers,** 28475 Witherspoon Dr, Novi, MI 48377, United States, +1-248-247-6042, WhatsApp +1 (248) 275-1133, info@medwinpublishers.com

© 2026, by the Authors. The articles published from this journal are distributed to the public under "**Creative Commons Attribution License**" (https://creativecommons.org/licenses/by/4.0/). Therefore, upon proper citation of the original work, all the articles can be used without any restriction or can be distributed in any medium in any form.